Monthly Notices of the ROYAL ASTRONOMICAL SOCIETY

MNRAS **436,** 3321–3330 (2013)
Advance Access publication 2013 October 23

doi:10.1093/mnras/stt1808

# The X-ray spectrum and spectral energy distribution of FIRST J155633.8+351758: a LoBAL quasar with a probable polar outflow

Robert C. Berrington,[1⋆] Michael S. Brotherton,[2] Sarah C. Gallagher,[3] Rajib Ganguly,[4] Zhaohui Shang,[5] Michael DiPompeo,[2] Ritaban Chatterjee,[6,2] Mark Lacy,[7] Michael D. Gregg,[8,9] Patrick B. Hall[10] and S. A. Laurent-Muehleisen[11]

[1]*Department of Physics and Astronomy, Ball State University, Muncie, IN 47306, USA*
[2]*Department of Physics and Astronomy, University of Wyoming, Laramie, WY 82071, USA*
[3]*Department of Physics and Astronomy, University of Western Ontario, London, Ontario N6A 3K7, Canada*
[4]*Department of Computer Science, Engineering, and Physics, University of Michigan-Flint, Flint, MI 48502, USA*
[5]*Tianjin Normal University, Tianjin 300387, China*
[6]*Department of Physics, Presidency University, 86/1 College Street, Kolkata 700073, WB, India*
[7]*North American ALMA Science Center, National Radio Astronomy Observatory, Charlottesville, VA 22903-2475, USA*
[8]*Physics Department, University of California, Davis, CA 95616, USA*
[9]*Institute of Geophysics and Planetary Physics, Lawrence Livermore National Laboratory, PO Box 808, L-413, Livermore, CA 94551-9900, USA*
[10]*Department of Physics and Astronomy, York University, Toronto, ON M3J 1P3, Canada*
[11]*Physics Division of Biological, Chemical, and Physical Sciences, Illinois Institute of Technology, Chicago, IL 60616, USA*

Accepted 2013 September 24. Received 2013 September 23; in original form 2013 May 24

## ABSTRACT

We report the results of a new 60 ks *Chandra X-ray Observatory* Advanced CCD Imaging Spectrometer S-array (ACIS-S) observation of the reddened, radio-selected, highly polarized 'FeLoBAL' quasar FIRST J1556+3517. We investigated a number of models of varied sophistication to fit the 531-photon spectrum. These models ranged from simple power laws to power laws absorbed by hydrogen gas in differing ionization states and degrees of partial covering. Preferred fits indicate that the intrinsic X-ray flux is consistent with that expected for quasars of similarly high luminosity, i.e. an intrinsic, dereddened and unabsorbed optical to X-ray spectral index of −1.7. We cannot tightly constrain the intrinsic X-ray power-law slope, but find indications that it is flat (photon index $\Gamma = 1.7$ or flatter at a >99 per cent confidence for a neutral hydrogen absorber model). Absorption is present, with a column density a few times $10^{23}$ cm$^{-2}$, with both partially ionized models and partially covering neutral hydrogen models providing good fits. We present several lines of argument that suggest the fraction of X-ray emissions associated with the radio jet is not large. We combine our *Chandra* data with observations from the literature to construct the spectral energy distribution of FIRST J1556+3517 from radio to X-ray energies. We make corrections for Doppler beaming for the pole-on radio jet, optical dust reddening and X-ray absorption, in order to recover a probable intrinsic spectrum. The quasar FIRST J1556+3517 seems to be an intrinsically normal radio-quiet quasar with a reddened optical/UV spectrum, a Doppler-boosted but intrinsically weak radio jet and an X-ray absorber not dissimilar from that of other broad absorption line quasars.

**Key words:** quasars: absorption lines – quasars: general – quasars: individual (FIRST J155633.8+351758) – X-rays: galaxies.

## 1 INTRODUCTION

A substantial fraction of quasars possess intrinsic high-velocity outflows along the line of sight, the most extreme of which are characterized by broad absorption lines (BALs): broad, blueshifted resonance absorption lines seen in the rest-frame ultraviolet. The dynamics of these intrinsic outflows appear to be the result of radiative acceleration (e.g. Arav, Korista & Begelman 1995; Ganguly et al. 2007; DiPompeo, Brotherton & De Breuck 2012b). Taken at face value, the ultraviolet BALs suggest absorbing column densities of $N_{\mathrm{H}} \sim 10^{20}$–$10^{21}$ cm$^{-2}$ in these outflows (Hamann, Korista & Morris 1993), although there is evidence that the actual column densities are much higher, the result of partial covering of the continuum

⋆ E-mail: rberring@bsu.edu

(e.g. Arav et al. 1999) or scattered light (e.g. Ogle et al. 1999) filling in what would otherwise be black, saturated absorption troughs.

The X-ray regime has supported the idea that the column densities towards BAL quasars are quite high. Green & Mathur (1996) argued more than a decade ago that *ROSAT* non-detections indicated column densities of greater than $N_{\rm H} \sim 10^{22}$ cm$^{-2}$, and deeper observations of BAL quasars by later X-ray telescopes indicate typical column densities of $N_{\rm H} \sim 10^{23}$ cm$^{-2}$ as well as objects with columns in excess of $10^{24}$ cm$^{-2}$ (recently tabulated by Punsly 2006).

While progress has been made in understanding some properties of BAL outflows (see e.g. Gallagher & Everett 2007), many aspects of their intrinsic nature remain poorly constrained. The relationship between the ultraviolet and X-ray absorbing material is not known for certain. The location, geometry, physical state and chemical abundance of the absorbing material are poorly constrained and model dependent. It is not yet known whether outflows are present in every quasar, and why their properties vary so dramatically (although there is a strong luminosity dependence, e.g. Ganguly et al. 2007).

X-ray investigations have provided some progress. In the X-ray regime, deep observations of individual BAL quasars with the *XMM–Newton* and *Chandra* observatories have led to a better understanding of the absorbing material. The general result seems to be that BAL quasars have underlying intrinsic X-ray properties consistent with those of unabsorbed quasars, and the absorber is complex requiring fitting with models featuring some combination of ionization and/or partial covering (Gallagher et al. 2006). Recent studies investigating BAL quasars versus radio-loudness favoured a geometric model to describe the observed properties, but could not explain strong polar BAL quasars or the deficit of FR II sources within BAL quasars (Shankar, Dai & Sivakoff 2008). The dependence of the physical nature of the BAL outflows on properties such as radio-loudness or the absorber ionization state needs to be observationally established to better understand these systems (see e.g. Dai, Shankar & Sivakoff 2012).

To date, nearly all of the BAL quasars with observed X-ray spectra beyond mere detections have been optically bright, blue and radio-quiet, displaying only high-ionization BALs (HiBALs); three exceptions are the cloverleaf quasar with low-ionization BALs (LoBALs), H1413+117 (e.g. Chartas et al. 2004), the LoBAL quasar Mrk 231 (Gallagher et al. 2002a; Braito et al. 2004) and the radio-loud BAL quasar PKS 1004+130 (e.g. Miller et al. 2006). Similar fractions of radio-loud and radio-quiet quasars display BALs quasars (e.g. Brotherton et al. 1998; Becker et al. 2000, 2001; Hewett & Foltz 2003; Shankar et al. 2008), although BALs are only very rarely seen in the spectra of powerful FR II radio-loud quasars (Gregg, Becker & de Vries 2006). LoBAL quasars are probably rarer than radio-loud BAL quasars, but so-called LoBAL quasars are also often reddened (e.g. Becker et al. 2000; Brotherton et al. 2001, Sprayberry & Foltz 1992, DiPompeo et al. 2012a), and the BAL troughs can effectively wipe out rest-frame ultraviolet light (e.g. Hall et al. 2002), making their true frequency difficult to determine accurately.

FIRST J155633.8+351758 ($z = 1.5008 \pm 0.0007$), hereafter FIRST J1556+3517, was originally discovered as a red stellar object associated with a radio source (Becker et al. 1997), and was identified as the first radio-loud BAL quasar based on its observed properties. We will discuss this classification later. Its spectrum is unusual, even for BAL quasars, displaying not only absorption from low-ionization species like Mg II, but also metastable Fe II species, garnering it the subclass of 'FeLoBAL' quasar. It is also one of the most optically polarized BAL quasars known (Brotherton et al. 1997), and is reddened by $A_{\rm V} \approx 1.6$ (Najita, Dey & Brotherton 2000). Furthermore, based on its radio variability, FIRST J1556+3517 can be identified as a BAL quasar seen close to jet on (Ghosh & Punsly 2007). The combination of extreme properties makes this quasar an interesting target to study at all wavelengths.

Brotherton et al. (2005) detected FIRST J1556+3517 at X-ray energies as part of an exploratory *Chandra* survey of radio-loud BAL quasars. All the quasars in the survey are X-ray faint compared to unabsorbed radio-loud quasars of similar luminosity. Previous studies by Miller et al. (2009) have confirmed that BAL quasars appear X-ray weak relative to their non-BAL quasar counterparts. Compared to other LoBAL quasars, however, FIRST J1556+3517 is relatively X-ray bright (0.0077 counts s$^{-1}$ with *Chandra* Advanced CCD Imaging Spectrometer S-array (ACIS-S) in the 0.35–8 keV energy band), making it a good target for deeper follow-up.

We report here the results of a new 60 ks ACIS-S observation of FIRST J1556+3517 with the *Chandra X-ray Observatory* (Section 2). We discuss the lack of long- and short-term variability in Section 3. We explore a variety of models to fit the X-ray spectrum (Section 4). Our new observations, in conjunction with other information from literature, allow us to comprehensively investigate the observed and intrinsic spectral energy distribution (SED) of FIRST J1556+3517 for the first time (Section 5). Finally, we discuss our results in the context of how this extreme quasar fits into our understanding of the broader population of BAL quasars and summarize our conclusions (Section 6). We assume a cosmology defined by ($\Omega_0$, $\Omega_\Lambda$, $h_{100}$) = (0.30, 0.70, 0.70), where $h_{100} = H_0/100$ km s$^{-1}$ Mpc$^{-1}$. Unless otherwise noted, error bars are $1\sigma$, and power-law slopes ($\alpha$) are defined by the equation $F_\nu \propto \nu^\alpha$.

## 2 OBSERVATIONS AND DATA REDUCTION

We started the observations of our target on 2006 June 2 at 09:25:43 GMT (MJD: 538 88.392 87) with the *Chandra X-ray Observatory* ACIS-S3 in very faint (VFAINT) mode. We measured a total of 531 photons from the program object in the 0.5–10 keV energy band over the 60 ks exposure time for a photon rate of $8.85 \pm 0.38 \times 10^{-3}$ photons s$^{-1}$. Fig. 1 shows the counts per second received versus the exposure time for the 0.3–2, 2–10 and 0.3–10 keV energy bands. The data were initially processed using the standard *Chandra* X-ray Center pipeline software. Only the level 1 events file was used. Additional processing was carried out with the `acis_process_events` procedure of the CIAO 3.4 software. Additional processing included removal of pixel randomization, and selection of good Advanced Satellite for Cosmology and Astrophysics grades (0,2,3,4,6) and good status (ignoring the bits indicating afterglow events). The background light curve was inspected for temporal fluctuations. Fortunately, none of the 60 ks exposure time was lost to flaring. The VFAINT 5 × 5 event island was used to improve the filtering of the background for cosmic rays. From the calculated photon rate, the estimated photon pile-up is <1 per cent. As a precautionary measure, 'bad' events filtered by the above-mentioned reduction procedure were visually inspected to see if any of the source X-rays were rejected. None was found.

The source photons were extracted by the `psextract` procedure from a circular aperture with a 5 arcsec radius centred on the source. The background spectrum was taken from a concentric annulus void of any visible emission sources or deficits with an inner radius of 10 arcsec and an outer radius of 20 arcsec. The redistribution matrix (rmf) and auxiliary response file (arf) were constructed using

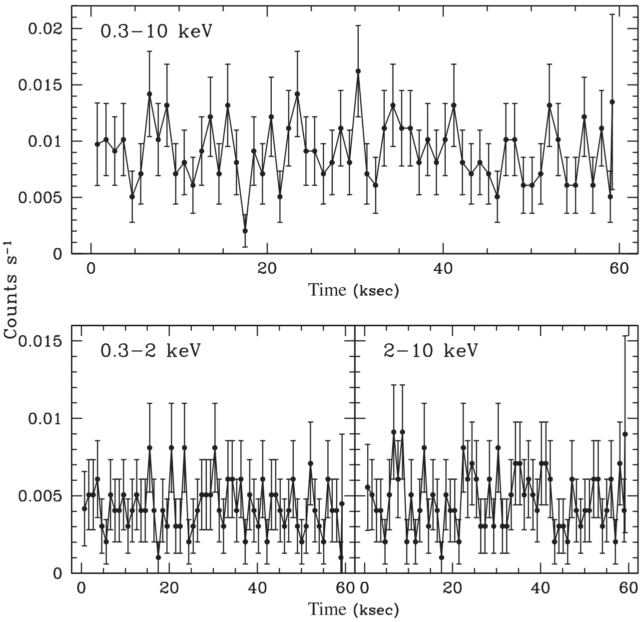


**Figure 1.** X-ray light curve for FIRST J1556+3517. Counts are binned in ∼1 ks intervals, and energy bands are labelled in the top-left corner of each panel. All error bars are 1$\sigma$ error bars as estimated by $\sqrt{n}$.

the standard procedure in CIAO 3.4. For further spectral analysis in XSPEC (v. 12.3.1),[1] which is a detector independent, X-ray spectral-fitting program, the rmf and arf energy grids were matched. Energy ranges were restricted to the 0.5–10 keV range as below 0.5 keV the calibration is uncertain. Note that above 8.0 keV the effective area drops steeply and the particle background increases, but for our analyses restricting the energy range to 0.5–8 keV had no effect on our conclusions.

## 3 VARIABILITY

A visual inspection of the X-ray light curves (Fig. 1) did not reveal any significant short-term variability. To quantify any possible sub-60 ks variability, we applied a Kolmogorov–Smirnov test to the temporal cumulative photon count in the soft (0.3–2 keV), hard (2–10 keV) and total energy (0.3–10 keV) energy bandpass. We found the photon rate to be consistent with a constant photon flux for the soft, hard and total energy bandpasses at the >90 per cent level.

Brotherton et al. (2005) estimated the photon rate to be $7.7 \pm 1.3 \times 10^{-3}$ photons s$^{-1}$ in the 0.35–8 keV energy band from a 5 ks *Chandra* observation which started on 2000 May 20 at 10:51:30 GMT (MJD: 51 684.452 43). They calculated an unabsorbed 0.35–8 keV flux of $6.5 \times 10^{-14}$ erg cm$^{-2}$ s$^{-1}$ using PIMMS[2] with a photon index $\Gamma = 1.7$, and assuming a Galactic column density of $2.0 \times 10^{20}$ cm$^{-2}$. However, the most appropriate effective area for cycle 1 was not employed in their flux calculation. We have carried out a better flux estimate using a more recent version of PIMMS with an effective area more suitable (cycle 3) for the Brotherton et al. (2005) observations. Our improved flux estimation using the same assumptions mentioned previously is $5.1 \pm 0.9 \times 10^{-14}$ erg cm$^{-2}$ s$^{-1}$. In this work, we also employed PIMMS with a suitable effective area and the same assumptions of the Brotherton et al. (2005) observations for consistency. Our new observation indicates a constant count rate of $8.9 \pm 0.4 \times 10^{-3}$ photons s$^{-1}$ over the 60 ks exposure in the 0.5–10 keV energy band, and any intrinsic variability is negligible compared to the photon statistics. Our measurement corresponds to an unabsorbed flux of $7.1 \pm 0.3 \times 10^{-14}$ erg cm$^{-2}$ s$^{-1}$ in the 0.35–8 keV energy range using the same assumptions of $\Gamma = 1.7$ and Galactic column. This indicates a photon arrival rate that is higher than the previous epoch at a 2.2$\sigma$ level, only a marginal difference. Evidence for long-term X-ray variability is not conclusive.

We also note that FIRST J1556+3517 was observed a total of four times with the *XMM–Newton* observatory. All observations were inspected and suffered from flaring events. The portions of the observations suitable for data extraction were $\lesssim$20 per cent of the total observation time, and did not place further constraints on either the long-term or short-term X-ray variability.

## 4 EXPLAINING THE X-RAY SPECTRUM OF FIRST J1556+3517

There exist several explanations for the X-ray properties of FIRST J1556+3517, as discussed by Brotherton et al. (2005). They rejected the simplest idea that FIRST J1556+3517 is an intrinsically normal quasar seen through a large column density of neutral hydrogen. Brotherton et al. (2005) used the radio–X-ray correlation (Brinkmann et al. 2000) to estimate the intrinsic X-ray flux, and, comparing that result to the observed *Chandra* count rate, determined that the observed X-rays were suppressed by a factor of 49. This reduction in X-rays, if attributed to a neutral hydrogen absorber, requires a column density of $6.0 \times 10^{23}$ cm$^{-2}$. This large of a column, however, would result in an extremely large hardness ratio (HR). The HR is defined as follows:

$$\mathrm{HR} = \frac{H - S}{H + S}, \tag{1}$$

where $S$ and $H$ are the total photon count in the soft band (0.35–2 keV) and the hard band (2–8 keV), respectively. Brotherton et al. concluded that the observed HR of $-0.1 \pm 0.2$ is incompatible with that expected from a normal quasar absorbed by neutral hydrogen with column density $\sim 10^{23}$ cm$^{-2}$.

They preferred more complex explanations that reduce the observed X-ray flux and not resulting in an HR that is inconsistent with observations. These include: emission from an unobscured jet (mentioned below), an ionized absorber, a partially covering neutral absorber or scattering/reflection. Now, with a spectrum with more than 500 counts, we can revisit the proposed explanations in more detail. We start with simple models and proceed to test the more complex alternatives.

The best-fitting parameters are determined by minimizing the sum of the squares of the deviations ($\chi^2$) with Marquardt–Levenberg optimization. We restrict our fitting range to 0.5–10 keV, and assume a Galactic column density of $2.0 \times 10^{20}$ cm$^{-2}$ for all models (Dickey & Lockman 1990), with relative abundances defined by Anders & Grevesse (1989) and the cross-sections of Morrison & McCammon (1983). A study of the brightness temperature and radio variability (time-scale of ∼1 year) of FIRST J1556+3517 by Ghosh & Punsly (2007) supports the presence of a beamed radio source. Because of this likelihood, the use of the radio-X-ray correlation to estimate the intrinsic X-ray flux is suspect and therefore we prefer to permit normalizations to vary freely.

[1] http://heasarc.gsfc.nasa.gov/docs/xanadu/xspec/index.html
[2] http://cxc.harvard.edu/toolkit/pimms.jsp

### 4.1 Power-law and neutral absorber models

We start with a very simple model to confirm the presence of absorption. We fit a power-law model plus only Galactic extinction. The fit quality was poor (with a reduced $\chi^2$ or $\chi^2/\nu = 1.53$ where $\nu$ is the number of degrees of freedom), and overpredicted the photon flux for energies $<1.5$ keV. Model fits are classified as statistically significant fits for reduced $\chi^2 \lesssim 1.0$. Henceforth, the quality of a model fit will be reported in terms of their reduced $\chi^2$ unless otherwise noted. The best-fitting model resulted in a flat photon index of $\Gamma = 0.7^{+0.05}_{-0.06}$ where $\Gamma$ is defined by $N(E) = KE^{-\Gamma}$ photons s$^{-1}$ cm$^{-2}$ keV$^{-1}$.

To highlight the presence of absorption, we fit a power-law model only to the observed frame 2–5 keV energy band (Fig. 2). The resulting fit favoured a slightly softer photon index of $\Gamma = 0.85^{0.38}_{-0.23}$, but is no better than previous fit ($\chi^2/\nu = 1.36$). Fig. 2 shows the inability of the power-law model to accurately fit the $\lesssim$1.5 keV energy range, where the soft photons fall far below. This result supports the conclusion of Brotherton et al. (2005) that the X-rays suffer absorption.

Next, we fixed the power-law photon index at $\Gamma = 1.7$ from the average photon index of radio-loud quasars (Brotherton et al. 2005), but added a neutral hydrogen column absorber at the quasar redshift. Fig. 3 shows the best-fitting neutral absorber model with a the photon index fixed at $\Gamma = 1.7$. We note that assuming a typical, softer radio-quiet quasar photon index would be even more problematic than what we find for the radio-loud case. Allowing both the intrinsic neutral absorber column density and the normalization to vary freely, the resulting best-fitting model is only marginally better ($\chi^2/\nu = 1.32$), failing to fit in particular the lowest energies. If we let the intrinsic photon index vary freely, then the best-fitting model is improved ($\chi^2/\nu = 0.98$). This best-fitting model is statistically as significant as some of the more complex models we investigate below, but requires an extremely flat, and perhaps unrealistic, photon index of $\Gamma = 1.2 \pm 0.1$. The parameters describing both fits are shown in Table 1.

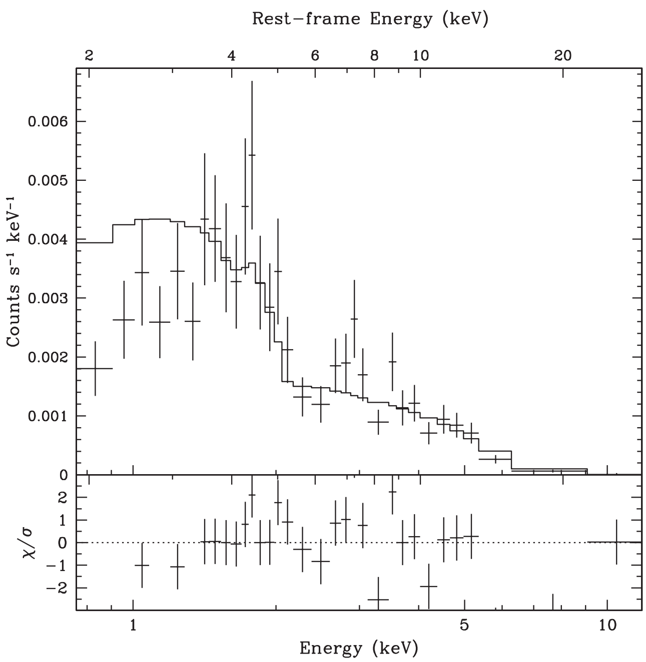


**Figure 2.** The best-fitting power-law model for the observed energies 2–5 keV. The model includes a Galactic column density of $2.0 \times 10^{20}$ cm$^{-2}$. The lower panel shows the normalized deviations ($\chi/\sigma$) to the of the bin values from the best-fitting model normalized to observational error bars ($\sigma$). The panel range is selected to show the deviations of the points within the 2–5 keV energy range. The missing values reflect deviations outside the range of the panel. This model consistently overpredicts the X-ray photon flux for energies $\lesssim$1.3 keV. Observed energies are given along the bottom *x*-axis, and rest-frame energies are given along the top axis of both panels.

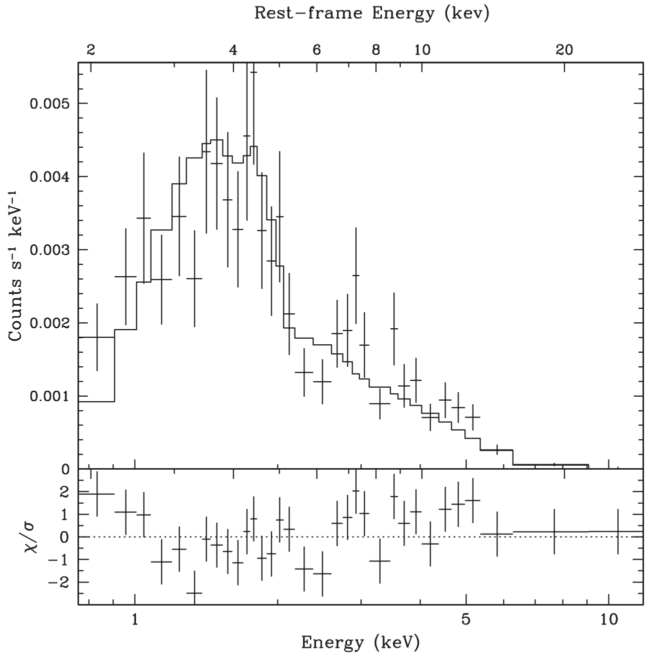


**Figure 3.** The best-fitting neutral absorber model. The model includes a Galactic column density of $2.0 \times 10^{20}$ cm$^{-2}$. The lower panel shows the normalized deviations ($\chi/\sigma$) to the of the bin values from the best-fitting model normalized to observational error bars ($\sigma$). The panel range is selected to show the deviations of the points within the 0.8–10 keV energy range. The missing values reflect deviations outside the range of the panel. This model fails to accurately predict the X-ray photon flux for energies $\lesssim 1$ keV. Observed energies are given along the bottom *x*-axis, and rest-frame energies are given along the top axis of both panels.

### 4.2 Partially covering neutral absorber

The neutral absorber model was unable to reproduce the observed soft X-ray photons in the observed spectrum with a realistically steep intrinsic photon index (e.g. $\Gamma = 1.7$). By allowing the neutral absorber to cover only a fraction of the emitted X-ray spectrum, the uncovered fraction of the X-ray emitter allows some soft photons to reach the observer unimpeded. By varying the covering fraction and the absorber column density, both the total X-ray flux and HR may be adjusted to fit the spectrum. The partial covering neutral absorber is modelled by the `zpcfabs` model. Table 1 summarizes our best-fitting models, both fixing $\Gamma = 1.7$ as well as letting it vary, with a similar or better $\chi^2$ as the partially ionized absorber models. The total column densities for these models is of the order of $10^{23}$ cm$^{-2}$ with covering fractions of 0.87 and 0.81, respectively. The best-fitting partially covering neutral absorber model for a best-fitting photon index $\Gamma = 1.4 \pm 0.2$ is shown in Fig. 4.

### 4.3 Partially ionized absorbing models

Partially ionized absorbers are capable of significantly reducing X-ray flux without creating an excessively hard source. To test such

**Table 1.** Model parameters.

| Property[a] | | Model 1 | Model 2 |
|---|---|---|---|
| | | Neutral absorber | |
| $N_{\rm H}$ ($10^{22}$ cm$^{-2}$) | = | $7.0^{+1.0}_{-0.8}$ | $3.6^{+1.1}_{-0.9}$ |
| Norm | = | $2.2 \pm 0.2 \times 10^{-5}$ | $1.2^{+0.2}_{-0.2} \times 10^{-5}$ |
| $\Gamma$ | = | 1.7 | $1.2 \pm 0.1$ |
| $(\chi^2/\nu)$ | = | 1.32(40.9/31) | 0.98(29.4/30) |
| | | Ionized absorber | |
| $N_{\rm H}$ ($10^{22}$ cm$^{-2}$) | = | $27.2^{+9.9}_{-8.5}$ | $37.5 \pm 10.8$ |
| $\xi$ (erg cm s$^{-1}$) | = | $620^{+357}_{-363}$ | $1056^{+669}_{-573}$ |
| $T_g$ (K) | = | $3 \times 10^4$ | $3 \times 10^4$ |
| $\frac{[\rm Fe/H]}{[\rm Fe/H]_\odot}$ | = | 1.0 | 1.0 |
| Norm | = | $1.2 \pm 0.1 \times 10^{-4}$ | $2.3 \pm 0.2 \times 10^{-4}$ |
| $\Gamma$ | = | 1.7 | 2.0 |
| $(\chi^2/\nu)$ | = | 1.07(32.2/30) | 1.39(41.8/30) |
| | | Partially covering neutral absorber | |
| $N_{\rm H}$ ($10^{22}$ cm$^{-2}$) | = | $14^{+3.0}_{-2.5}$ | $9.5^{+4.2}_{-4.1}$ |
| Covering fraction | = | $0.87 \pm 0.03$ | $0.81^{+0.07}_{-0.08}$ |
| Norm | = | $1.3 \pm 0.1 \times 10^{-4}$ | $6.0^{+4.1}_{-2.4} \times 10^{-5}$ |
| $\Gamma$ | = | 1.7 | $1.4 \pm 0.2$ |
| $(\chi^2/\nu)$ | = | 0.98(29.3/30) | 0.94(27.3/29) |

[a] All values are quoted for the rest frame. All fits include a Galactic column density of ($N_{\rm H} = 2.0 \times 10^{20}$ cm$^{-2}$). Errors included with each property are $1\sigma$ errors. Properties without errors were held fixed with model 1 having a photon index of value 1.7, and model 2 with alternate or varying photon index values.

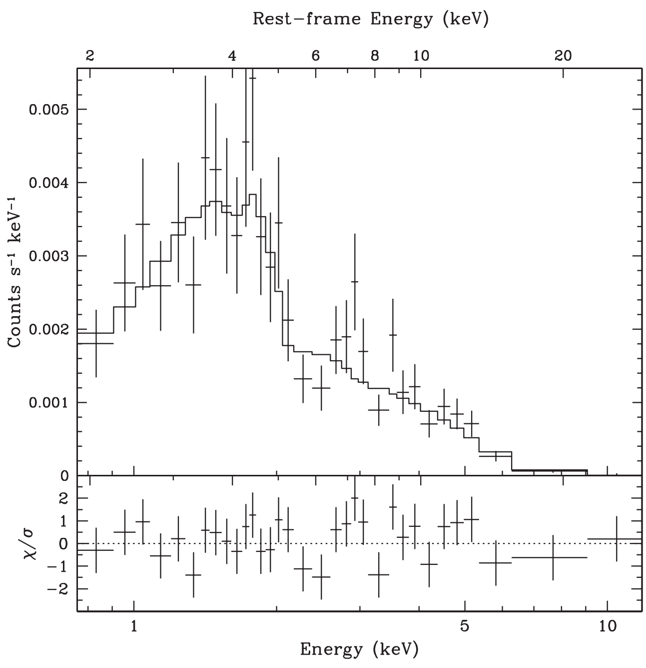


**Figure 4.** The best-fitting partially covering neutral absorber model. The intrinsic X-ray spectrum is assumed to be a power law with a photon index of $\Gamma = 1.4 \pm 0.2$. The parameters describing the best-fitting model are given in Table 1, model 2. The bottom panel and panel axes for both panels are the same as Fig. 2.

models, we applied the ionized absorber model, `absori`, provided in the XSPEC package.

We restricted the relative solar iron abundance to unity and held the gas temperature fixed at $\sim 3 \times 10^4$ K. Relative elemental abundances are defined by Anders & Grevesse (1989). The ionizing photon index was set at $\Gamma = 1.7$ initially. The absorber ionization state parameter $\xi$ as defined by Done et al. (1992) was allowed to vary freely. Typical values for our fits were $\xi \gtrsim 500.0$ erg cm s$^{-1}$. See Table 1 for exact values. Absorber ionization state is defined by the ionization parameter $\xi = L/nr^2$ of Done et al. (1992) where $L$ is the integrated incident luminosity from 5 eV to 300 keV and $r$ is the distance of the absorbing material of density $n$ from the illuminating source. Fig. 5 shows the best-fitting model ($\chi^2/\nu = 1.08$) to the observed X-ray spectrum. For these parameters, the column density for the ionized material required to match the observed spectrum is $3.7 \times 10^{23}$ cm$^{-2}$. We also fit a model using a fixed photon index of $\Gamma = 2.0$, similarly given in Table 1, which was worse ($\chi^2/\nu = 1.39$).

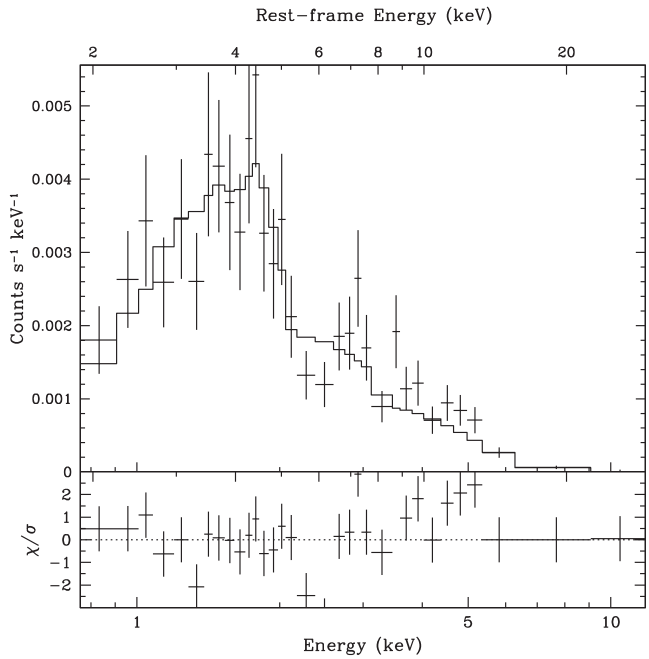


**Figure 5.** The best-fitting ionized absorber model. The intrinsic X-ray spectrum is assumed to be a power law with a photon index of $\Gamma = 1.7$. The parameters describing the best-fitting model are given in Table 1. The bottom panel is the same as the bottom panel of Fig. 2. Observed energies are given along the bottom $x$-axis. Rest-frame energies are given along the top axis of both panels.

To investigate the significance of the fit for the partially ionized absorber model over the neutral absorber model ($\xi = 0.0$ ergs cm s$^{-1}$), we test for the significance that the ionization parameter ($\xi$) is greater than 0 with the photon index $\Gamma$ as a free parameter. Our best-fitting models favoured values of $\Gamma \approx 1.3$, and values $\xi \approx 300$ erg cm s$^{-1}$. The partially ionized absorber model marginally improves the fit over a neutral absorber model ($\sim 2\sigma$) when photon indices are held fixed at values consistent with quasar observations (Green et al. 2009).

### 4.4 Scattering/reflection

Brotherton et al. (1997) showed that the polarization fraction of the optical continuum for FIRST J1556+3517 is $\gtrsim$13 per cent, and argued that the polarization mechanism was scattering either by dust or hot electrons. If the polarization mechanism is scattering by electrons, then both the optical and X-ray emission will be similarly scattered, and the minimum amount of the intrinsic X-ray flux scattered into the line of sight is expected to be $\sim$13 per cent. This would imply that the intrinsic X-ray flux is no greater than approximately eight times the observed X-ray flux.

Brotherton et al. (2005) argued for a ratio of $\sim$50 between the intrinsic and observed X-ray flux based on the radio–X-ray correlation, much larger than the factor of 8 deduced from electron scattering. They thus concluded that electron scattering was not the mechanism in operation, although it is also possible that the optical and X-ray geometries differ.

We note that in principle scattering need not appear differently in an unresolved source from partial covering. Some fraction of the light passes through or around an absorber. The partially covering neutral absorber models of the previous section result in acceptable fits, and are consistent with the $\sim$13 per cent polarization level. That is, in the case where the polarization efficiency is 100 per cent, both the optical and X-ray results may be explained by the same geometry. This would require that the intrinsic X-ray flux levels found for the partial covering models be plausible, which they are (see Section 5).

What about reflection from colder material? In general, the presence of an Fe K$\alpha$ line in a reflected X-ray spectrum depends on the ionization state of the reflecting material. With a possible rest-frame energy of 6.4 keV (neutral), 6.7 keV (He-like) and 6.96 keV (H-like), and an observed redshift of $z = 1.5008 \pm 0.0007$, we expect the Fe K$\alpha$ line to be observed at 2.6 keV (neutral), 2.7 keV (He-like) and 2.8 keV (H-like), respectively. Figs 2–4 show a possible emission feature centred at $\sim$2.9 keV, which has a rest-frame energy of 7.2 keV. If the observed feature is an Fe K$\alpha$ line it must be associated with outflowing material (at >99 per cent confidence). The possible calculated outflow velocities are $5.0 \pm 0.6 \times 10^4\,\mathrm{km\,s^{-1}}$ for a neutral Fe K$\alpha$, $2.7 \pm 0.6 \times 10^4\,\mathrm{km\,s^{-1}}$ for He-like and $1.6 \pm 0.6 \times 10^4\,\mathrm{km\,s^{-1}}$ for H-like. It is difficult to associate the likely candidates with the possible emission feature observed at $\sim$2.9 keV. This is not very compelling evidence for the existence of a reflected component. Higher quality observations are required to resolve this issue.

### 4.5 The possibility of jet X-rays

Alternatively, X-ray photons may be produced in the jet through synchrotron and/or inverse-Compton processes. Whether or not FIRST J1556+3517 is intrinsically radio-loud or radio-quiet, it is clearly associated with a compact, flat spectrum radio source that may signify a jet (Reynolds, Punsly & O'Dea 2013). However, we argue that the origin of X-rays from FIRST J1556+3517 are mostly of non-jet origin because of the following.

(i) Electrons that produce synchrotron emission at X-ray energies in the presence of an $\sim$1 G magnetic field (a reasonable assumption for $\lesssim$pc-scale jets of quasars, e.g. Ghisellini et al. 2010) have Lorentz factors ($\gamma$) of $\sim 10^6$ with characteristic variability time-scales for high-energy electrons radiating at X-ray energies from approximately minutes to hours. This variability is supported by numerous observations of blazars (e.g. Takahashi et al. 1996; Chiappetti et al. 1999; Fossati et al. 2000; Kataoka et al. 2000; Edelson et al. 2001). If there were a significant contribution from a jet, we would expect to observe variability during the 60 ks window shown in Fig. 1. But none is observed.

If the synchrotron emission component does extend to the X-ray band, it is usually expected that the synchrotron peak is at or below the X-ray frequencies (e.g. Landt et al. 2008). In that case, the X-ray spectrum should be steep ($\Gamma > 2$) in contrast to the observation. While a jet may contribute to the X-ray emission seen in FIRST J1556+3517, we find the flatter X-ray spectrum along with the lack of short-term variability is compelling evidence that the X-ray emission is not dominated by synchrotron emission from a jet.

(ii) The X-rays can also be produced by inverse-Compton scattering of seed photons by the relativistic electrons in the jet. The seed photons may be from outside the jet, such as thermal emission from the accretion disc or line emission from the broad-line region ('external Compton' or EC process), but may also originate from the synchrotron photons produced in the jet ('synchrotron self-Compton' or SSC process). Electrons responsible for generating SSC or EC X-rays are less energetic ($\gamma \sim 10^2$–$10^3$) and may have longer variability time-scales. Furthermore, the spectra of the X-ray photons produced by the SSC and EC processes can show flatter spectral slopes. Despite the possibility of not observing variability within a 60 ks window, we show that the observed X-ray flux in FIRST J1556+3517 is much larger than what is expected via SSC or EC processes in its pc-scale jet, and therefore unlikely to be dominated by emission from a jet.

Radio variability (time-scale of $\sim$1 yr) and the correspondingly high brightness temperature indicate the presence of a beamed jet aligned within 14° of the line of sight (Ghosh & Punsly 2007). Monte Carlo simulations of the correlation between viewing angle and radio power-law spectral indices for BAL quasars supports a similar viewing angle ($\sim$16°) from the aforementioned radio power-law slopes (DiPompeo et al. 2012b). If we assume that the radio core has an angular size of $\sim$1 mas (Jiang & Wang 2003 report an upper limit of 20 mas), the spectral index of optically thin synchrotron emission $\alpha = 0.75$ and the Doppler factor of 4 from Ghosh & Punsly (2007), then the estimated SSC flux of the jet associated with FIRST J1556+3517 (using equation 1 from Ghisellini et al. 1993) is $\sim 10^{-21}\,\mathrm{erg\,cm^{-2}\,s^{-1}}$. Where we have assumed energetic isotropic electrons well described a power-law energy distribution entrained within a tangled, homogeneous magnetic field, a spherically symmetric moving jet (see Ghisellini et al. 1993), and an observed frequency similar to the self-absorption frequency to account for the flat radio spectrum of the core emission. This flux value is many orders of magnitude lower than the observed *Chandra* X-ray flux ($\sim 10^{-14}\,\mathrm{erg\,cm^{-2}\,s^{-1}}$). Therefore, SSC emission associated with the jet cannot explain the observed X-ray properties, and is unlikely to be the dominant source of X-ray emission.

In most quasar jets the external photon field energy density is within a factor of $\leq$100 of energy density of the magnetic field (e.g. Ghisellini et al. 2010; Giommi et al. 2012). Hence, the EC radiation is within a factor of $\leq$100 of the SSC emission. However, as mentioned above, the estimated SSC flux is seven orders of magnitude smaller than the observed *Chandra* X-ray flux. Therefore, the EC X-rays will also be much smaller (approximately five orders of magnitude) than observed.

(iii) If there is a significant contribution of jet emission in the X-rays, it is likely that the optical–IR (OIR) emission will also be dominated by jet synchrotron emission(e.g. Chatterjee et al. 2008; Marscher et al. 2008; Jorstad et al. 2010; Marscher et al. 2010; Agudo et al. 2011; Bonning et al. 2012). In that case the OIR emission will be significantly polarized. However, Brotherton et al. (1997) showed that the emission lines observed in the optical are polarized at the same level as the optical continuum which strongly suggests that the observed polarization is a result of scattering. Hence, a synchrotron explanation for the polarization of the OIR emission is not required and, in fact, not likely.

(iv) It is evident from the SED that the X-ray emission in FIRST J1556+3517 is lower than what is expected from a non-BAL radio-quiet quasar with similar optical/UV emission. This is consistent with our conclusion that the jet does not contribute significantly to the X-ray band in this object.

Studies of the distribution of radio–X-ray power-law slopes ($\alpha_{\rm rx}$) of AGN with known jets indicates that the cores of flat radio spectrum quasars have an $\alpha_{\rm rx}$ centred on a value of 0.5 (Marshall et al. 2005) for non-simultaneous observations, and is distributed differently than the mean value of $-0.9$ for the extended emission associated with the jet (Marshall et al. 2005; Sambruna et al. 2006). Our calculated intrinsic $\alpha_{\rm rx} = -0.7$ places FIRST J1556+3517 between the core and jet distributions, possibly indicating that some of the observed X-ray spectrum has a jet origin. However, jet models are well described by simple power law or power law with neutral absorber models. If we accept the neutral absorber model, then the best-fitting observed photon index $\Gamma$ is uncharacteristically flat for radio-quiet quasars. For typical $\Gamma$ values, the neutral absorber model poorly describes the X-ray spectrum, and favours more complicated models not typical of jet model fits (Sambruna et al. 2006).

While a comparison of our observations to detailed observations of jets by Marshall et al. (2005) and Sambruna et al. (2006, 2007) indicate that FIRST J1556+3517 is consistent with the most extreme knots, and cannot rule out the possibility that a jet may be a significant contributor to the observed X-ray spectrum, we find it improbable, and find the arguments concerning the lack of X-ray variability presented in Section 3 and the arguments presented above compelling.

### 4.6 Analysis summary

We confirm the results found by Brotherton et al. (2005) that an absorber is present, but a simple neutral absorber alone with a photon index like that of normal quasars cannot accurately reproduce the observed X-ray spectrum. The best-fitting neutral absorber model required a column density of $>6.8 \times 10^{22}\,{\rm cm^{-2}}$ if the photon index is fixed at $\Gamma = 1.7$. The neutral absorber model requires an intrinsic X-ray slope that is extremely flat ($\Gamma = 1.2$) to achieve a good fit. This photon index is approximately a $2\sigma$ deviation from the mean photon index observed for bright X-ray sources (George et al. 2000; Tozzi et al. 2006) placing it on the tail of the distribution for photon indices and therefore unlikely. We prefer the more complex models.

Of the other models explored, several gave reasonable fits to the observed X-ray spectrum. The first of these is the partially ionized absorber. While this model does not help to explain other features like the presence of polarized light in the optical spectrum, it is plausible. In this case, there is strong absorption with column densities $N_{\rm H} \approx 4.0 \times 10^{23}\,{\rm cm^{-2}}$.

We prefer the partially covering neutral absorber model, as it provides a similarly good fit, but may also have the following additional explanatory power. Partial covering is consistent with the presence of scattered light, which also explains the high optical polarization. The best-fitting values are smaller, but still high, with column densities of $N_{\rm H} \approx 1.0 \times 10^{23}\,{\rm cm^{-2}}$ and a covering fraction of ~85 per cent. The inferred intrinsic X-ray flux level will be considered in light of the total SED in the next section.

## 5 SPECTRAL ENERGY DISTRIBUTION

With our *Chandra* observations, FIRST J1556+3517 has now been observed across more than eight orders of magnitude in frequency, from radio wavelengths through X-ray energies. Fig. 6 presents the SED. X-ray observations on the right are from this paper, with individual points representing flux bins as in previous figures.

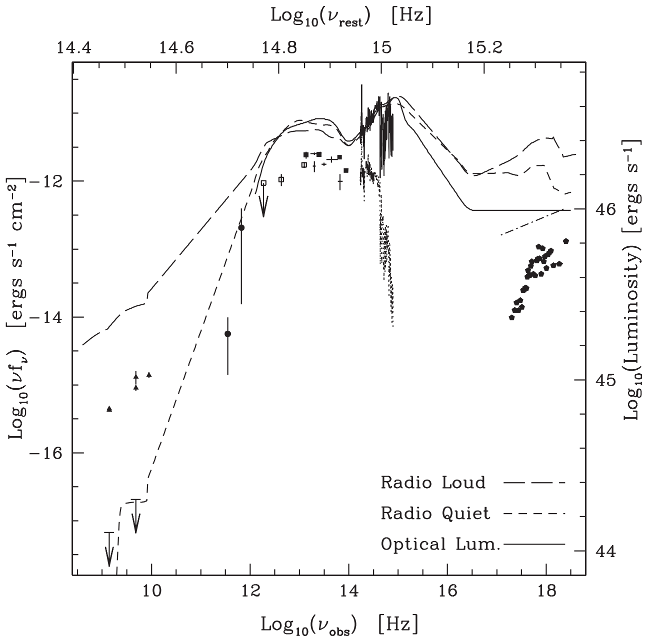


**Figure 6.** SED for FIRST J1556+3517. The optical luminous (solid) SED of Richards et al. (2006), the radio-loud (long dashed) and radio-quiet (dashed) Elvis et al. (1994) SEDs are shown. Data points are from the literature (for specific details see Section 5), and include both the reddened (dotted) and dereddened (thin solid) optical spectrum of Najita et al. (2000). The dereddened total-light spectrum assumes $A_V \approx 1.6$ and an SMC dust model. Note the Elvis SEDs are approximately seven times brighter than the predicted intrinsic X-ray luminosity of the partially covering neutral absorber model (dot–dashed). The SEDs are normalized to the dereddened optical spectrum, and all frequencies are observed frequencies. All error bars shown are $1\sigma$ error bars, and the detection limit shown at $\log_{10}(\nu) \approx 12.2$ is a $3\sigma$ detection limit. The two radio upper limits are the radio emission values corrected for beaming (see Ghosh & Punsly 2007). The top and bottom axes give the base-10 logarithm of the photon frequency in the rest frame and the observed frame, respectively. The left axis represents the observed flux, and the right axis represents the observed luminosity in units of $\log_{10}({\rm erg\,s^{-1}})$.

Continuing left to lower frequencies is the observed optical (Keck spectrum; Brotherton et al. 1997), the near-infrared (Kitt Peak spectrum; Najita et al. 2000), the mid-infrared (*Infrared Space Observatory*; Clavel 1998), the far-infrared (*Spitzer*, Farrah et al. 2007; and *Wilkinson Microwave Anisotropy Probe*, DiPompeo et al. 2013), the millimetre (Submillimetre Common-User Bolometer Array on James Clerk Maxwell Telescope; Lewis, Chapman & Kuncic 2003) and the radio [Green Bank Telescope, Gregory & Condon 1991; the Very Large Array (VLA) Faint Images of the Radio Sky at Twenty-cm (FIRST) Survey, Becker, White & Helfand 1995; and the VLA, DiPompeo et al. 2011].

In addition to the observed SED, we make corrections in three regimes to present an estimate of the intrinsic SED. In the X-ray regime, we show the intrinsic unabsorbed power law of our preferred partially covered neutral absorber model. In the optical/near-infrared regime, we use the total light spectrum from Najita et al. (2000), dereddened by 1.6 visual magnitudes of extinction using an extinction law appropriate for the Small Magellanic Cloud (SMC), which provides a final spectral index of $-0.5$, matching average quasar spectra. This is consistent, certainly at the level of our SED plotted here on a log–log scale, with all the estimates of the reddening (Brotherton et al. 1997; Clavel 1998; Najita et al. 2000), which are all $A_V \sim 1.6$. Finally, in the radio regime, we show the correction for Doppler beaming based on the lower limit to the Doppler factor of 4 from Ghosh & Punsly (2007) (assuming an intrinsic radio spectral index of 0). For reference, the average radio-loud and radio-quiet quasar SEDs of Elvis et al. (1994) representative of lower luminosity quasars and the optically luminous quasar SED of Richards et al. (2006), a better match to FIRST J1556+3517, are scaled to match the dereddened optical flux and are also shown in Fig. 6. We note that we in particular matched the dereddened spectrum in the rest-frame optical where issues with polarization and BALs are minimized, and that the slope matched well with those of the SEDs.

A few points need to be mentioned. First, Zhou et al. (2006) and Ghosh & Punsly (2007) have shown that a class of BAL quasars based on radio source variability and brightness temperature arguments appear to be consistent with close to pole-on views, and hence polar outflows. This conclusion is supported by earlier arguments put forward by Becker et al. (2000) for a variety of outflow orientations of radio-selected BAL quasars based on a range of radio spectral indices consistent with both polar and edge-on geometries. More recent studies by DiPompeo et al. (2012a) compared the radio spectral indices and viewing angles of BAL quasars with unabsorbed quasars. Their analysis confirms a large overlap in the viewing angle distribution of both samples with both distributions extending to the jet axis supporting the existence of BAL quasars with polar outflows. The SED of FIRST J1556+3517 shows a flat radio spectrum consistent with that of a pole-on source. Ghosh & Punsly (2007) specifically identify FIRST J1556+3517 as close to pole-on, with a jet angle to the line of sight less than $14^{\circ}$ and a minimum Doppler factor of 4.

These considerations are relevant to the classification of FIRST J1556+3517 as a radio-loud quasar, and in understanding its X-ray properties. Becker et al. (1997), in fact, claimed this object as the first radio-loud BAL quasar, which is based on its apparent observed properties. One of the ways to classify radio-loudness is by using $\log_{10}(R^{*})$, the ratio of rest-frame 5 GHz to 2500 Å flux, with unity separating the classes (Stocke et al. 1992). Becker et al. reported $\log_{10}(R^{*}) > 3$, based on the observed optical and radio data. Najita et al. (2000) revised the $\log_{10}(R^{*})$ value to 0.9 based on dereddening the optical spectrum. If we additionally correct the radio data for beaming based on the Doppler factor and assume a flat radio spectrum as observed, we find that $\log_{10}(R^{*}) < -0.9$ and is consistent with radio-quiet quasars. Radio-quiet quasars are not radio silent, and have been observed to have relativistic jets and evidence of beaming like this before (Falcke, Patnaik & Sherwood 1996; Blundell, Beasley & Bicknell 2003; Wang et al. 2006). Making the beaming correction places the upper limits on the Elvis et al. (1994) radio-quiet quasar SED.

Gallagher et al. (2006) found LoBAL quasars to be optically reddened and more deficient in observed X-rays than quasars showing only HiBALs, and we see similar behaviour in FIRST J1556+3517; the target of our study is reddened and is X-ray deficient with apparent absorbing column densities $N_{\rm H} > 10^{23}\,{\rm cm^{-2}}$ (from our preferred models shown in Table 1). However, a study by Streblyanska et al. (2010) found that LoBAL quasars have lower column densities ($N_{\rm H} < 10^{22}\,{\rm cm^{-2}}$) than HiBAL quasars. Their conclusion may have been biased by the selection of X-ray bright BAL quasars with relatively high S/N spectra suitable for X-ray spectral analysis.

In the case of FIRST J1556+3517, we can directly determine the intrinsic X-ray brightness relative to the optical. After the corrections for optical/UV dereddening and X-ray absorption for our favoured reddening values and X-ray model, our intrinsic $\alpha_{\rm ox} = -1.7$. We define $\alpha_{\rm ox}$ to be the spectral index of a power-law between the monochromatic luminosity $L_{\nu}$ at the rest-frame optical 2500 Å and X-ray 2 keV (in ${\rm erg\,s^{-1}\,Hz^{-1}}$), or

$$\alpha_{\rm ox} = \frac{\log_{10}[L_{\nu}(2500\,\text{Å})] - \log_{10}[L_{\nu}(2\,{\rm keV})]}{\log_{10}[\nu(2500\,\text{Å})] - \log_{10}[\nu(2\,{\rm keV})]}. \quad (2)$$

The intrinsic $\alpha_{\rm ox}$ value is clearly smaller than expected for either the radio-loud or radio-quiet quasar SEDs of Elvis et al. (1994), by nearly an order of magnitude, but those SEDs were constructed for lower luminosity quasars. Using a more up-to-date result for the dependence of $\alpha_{\rm ox}$ on luminosity for radio-quiet quasars (Steffen et al. 2006), we calculate that FIRST J1556+3517 should have $\alpha_{\rm ox} = -1.73 \pm 0.35$. This is not far from our estimate and is consistent with our new observations and the optically luminous SED of Richards et al.

Other apparently pole-on BAL quasars have been observed at X-ray energies. A study by Wang et al. (2008) of four randomly selected polar BAL quasars using *XMM–Newton* detected two of them. The four quasars were selected randomly from a sample of eight BAL quasars pulled from the Sloan Digital Sky Survey quasar catalogue (York et al. 2000). The brightness temperatures were determined from their large radio band variability and far exceeded the inverse Compton limit ($10^{12}$ K). This was taken as compelling evidence for the presence of a relativistic beamed jet towards the observer (Zhou et al. 2006). These two detections show no clear evidence for X-ray absorption from neutral hydrogen, and the limit of one of the non-detections is also consistent with no absorption. The final non-detection, of FIRST J210757−062010, an FeLoBAL quasar, is likely significantly absorbed. They conclude, within the limits of their data, that any absorption if present must be complex (e.g. an ionized or partially covering absorber) or that there may be X-rays contributed from a radio jet outside the BAL region.

We can also consider the SEDs of quasars displaying BALs more generally, too. Gallagher et al. (2007) examined the SEDs of 38 BAL quasars, primarily bright blue radio-quiet BAL quasars from the Large Bright Quasar Survey (LBQS; Hewett, Foltz & Chaffee 1995, 2001). They noted that BAL quasars have optical to mid-infrared fluxes similar to those of normal quasars, although for a larger sample and more careful comparison, BAL quasars appear more likely to have a small mid-infrared excess (DiPompeo et al. 2013). Farrah et al. (2007) suggested that FeLoBAL quasars in particular have far-infrared excesses characteristic of enhanced star formation. Lazarova et al. (2012) found inconclusive evidence that far-IR luminosities of LoBAL quasars differ from non-LoBAL quasars, but did suggest that the IR-luminous LoBAL quasars have pronounced star formation rates in comparison to their non-LoBAL counterparts possibly implying a brief period during the LoBAL phase that quenched star formation rates to normal non-LoBAL levels. FIRST J1556+3517 appears to have an excess based on the observed data, but after dereddening the optical and scaling, the mid-infrared is deficient compared to the Elvis et al. and Richards et al. SEDs.

To summarize, we have assembled the observed SED of FIRST J1556+3517 and made corrections to obtain the intrinsic SED. We can now characterize this FeLoBAL quasar as a quasar consistent with a polar outflow and a normal intrinsic $\alpha_{\rm ox}$ for its luminosity. The radio emission is consistent with a beamed radio-quiet quasar. The mid and far-infrared fluxes are below average relative to the dereddened the optical emission, suggesting that the dust covering fraction and the star formation rate are not enhanced relative to the typical quasar.

## 6 CONCLUSIONS

We can reach a few conclusions about FIRST J1556+3517: the X-rays suffer absorption from an intervening column of the order of a few times $10^{23}$ cm$^{-2}$ or less, the absorption is likely complex (e.g. partial covering or partial ionization), and the intrinsic X-ray level is consistent with that of radio-quiet quasars of similar optical luminosity. These conclusions are similar to those that have been reached for most other BAL quasars (mostly HiBAL quasars) with deep X-ray observations. The absorber, while possessing a substantial column density, is not Compton-thick.

Of the satisfactory models we fit to our spectrum, we have a preference for the neutral absorber with partial covering. From the ultraviolet iron absorption, we know that very low ionization material is along the line of sight. We also know that there is significant scattered light present based on the spectropolarimetry of Brotherton et al. (1997), and scattered light may be interpreted as partial covering. Now that we understand FIRST J1556+3517 is a beamed luminous radio-quiet quasar, and that our determination of the intrinsic X-rays is consistent with this classification, we can explain the partial covering of the X-ray absorber and the optical polarization results simultaneously with electron scattering. Testing this idea will require knowledge of the X-ray polarization. Still, we make the suggestion that partial covering of the X-ray source is present and represents a manifestation of non-axisymmetric equatorial electron scattering around a polar outflow seen at a small angle.

The polar-outflow BAL quasars show the full range of ionization, with HiBALs, LoBALs and FeLoBALs, and no one has yet identified any clear distinguishing features from other BAL quasars aside from their radio properties. Their luminosities and BAL terminal velocities fall among those of other BAL quasars (Ganguly & Brotherton 2008), within the envelope thought to indicate radiative acceleration. They may be differently driven, but there is as yet no solid evidence to support that. Outflow along the jet direction suggests other possible acceleration mechanisms (e.g. jet entrainment). Wang et al. (2008) suggested possible differing acceleration mechanisms for polar BAL quasars, but more recent studies disagree (DiPompeo et al. 2012a).

We have added FIRST J1556+3517 to the short but growing list of BAL quasars with spectroscopic observation in the X-ray band. In addition to the aforementioned LoBAL quasars Mrk 231, H1413+117 and radio-loud PG 1004+130, these other BAL quasars, all radio-quiet HiBAL quasars, include PG 1411+442, PG 1535+547 and PG 2112+059 (Gallagher et al. 2002b), PG 1115+080 (Chartas, Brandt & Gallagher 2003), APM 08279+5255 (Chartas et al. 2002), Q 1246−057 and SBS 1542+541 (Grupe, Mathur & Elvis 2003), UM 425 (Aldcroft & Green 2003), CSO 755, Q 0000−263, and RX J0911.4+0551 (Page et al. 2005). We have also added FIRST J1556+3517 to the shorter list of BAL quasars with high-quality SEDs all the way from radio to X-rays. These are a subset of the above, primarily the brightest and lowest redshift sources, which includes the PG quasars, APM 08279+5255, and Mrk 231 (see also Gallagher et al. 2007 for lower quality SEDs of 38 LBQS BAL quasars).

## ACKNOWLEDGEMENTS

We acknowledge support from *Chandra* Award No. GO6-7105X and from the US National Science Foundation through grant AST 05-07781 (MSB). ZS acknowledge support by NASA under grant NNG05GD03G issued through the Office of Space Science and by National Natural Science Foundation of China through grant 10643001. This work was performed under the auspices of the US Department of Energy by the University of California, Lawrence Livermore National Laboratory under Contract No. W-7405-Eng-48.

## REFERENCES

Agudo I. et al., 2011, ApJ, 726, L13
Aldcroft T. L., Green P. J., 2003, ApJ, 592, 710
Anders E., Grevesse N., 1989, Geochim. Cosmochim. Acta, 53, 197
Arav N., Korista K. T., Barlow T. A., Begelman, 1995, Nat, 376, 576
Arav N., Becker R. H., Laurent-Muehleisen S. A., Gregg M. D., White R. L., Brotherton M. S., de Kool M., 1999, ApJ, 524, 566
Becker R. H., White R. L., Helfand D. J., 1995, ApJ, 450, 559
Becker R. H., Gregg M. D., Hook I. M., McMahon R. G., White R. L., Helfand D. J., 1997, ApJ, 479, L93
Becker R. H., White R. L., Gregg M. D., Brotherton M. S., Laurent-Muehleisen S. A., Arav N., 2000, ApJ, 538, 72
Becker R. H. et al., 2001, ApJS, 135, 227
Blundell K. M., Beasley A. J., Bicknell G. V., 2003, ApJ, 591, L103
Bonning E. W. et al., 2012, ApJ, 756, 13
Braito V. et al., 2004, A&A, 420, 79
Brinkmann W., Laurent-Muehleisen S. A., Voges W., Siebert J., Becker R. H., Brotherton M. S., White R. L., Gregg M. D., 2000, A&A, 356, 445
Brotherton M. S., Tran H. D., van Breugel W., Dey A., Antonucci R., 1997, ApJ, 487, L113
Brotherton M. S., van Breugel W., Smith R. J., Boyle B. J., Shanks T., Croom S. M., Miller L., Becker R. H., 1998, ApJ, 505, L7
Brotherton M. S., Arav N., Becker R. H., Tran H. D., Gregg M. D., White R. L., Laurent-Muehleisen S. A., Hack W., 2001, ApJ, 546, 134
Brotherton M. S., Laurent-Muehleisen S. A., Becker R. H., Gregg M. D., Telis G., White R. L., Shang Z., 2005, AJ, 130, 2006
Chartas G., Brandt W. N., Gallagher S. C., Garmire G. P., 2002, ApJ, 579, 169
Chartas G., Brandt W. N., Gallagher S. C., 2003, ApJ, 595, 85
Chartas G., Eracleous M., Agol E., Gallagher S. C., 2004, ApJ, 606, 78
Chatterjee R. et al., 2008, ApJ, 689, 79
Chiappetti L. et al., 1999, ApJ, 521, 552
Clavel J., 1998, A&A, 331, 853
Dai X., Shankar F., Sivakoff G. R., 2012, ApJ, 757, 180
Dickey J. M., Lockman F. J., 1990, ARA&A, 28, 215
DiPompeo M. A., Brotherton M. S., De Breuck C., Laurent-Muehleisen S., 2011, ApJ, 743, 71
DiPompeo M. A., Brotherton M. S., Cales S. L., Runnoe J. C., 2012a, MNRAS, 427, 1135
DiPompeo M. A., Brotherton M. S., De Breuck C., 2012b, ApJ, 752, 6
DiPompeo M. A., Runnoe J. C., Brotherton M. S., Myers A. D., 2013, ApJ, 762, 111
Done C., Mulchaey J. S., Mushotzky R. F., Arnaud K. A., 1992, ApJ, 395, 275
Edelson R., Griffiths G., Markowitz A., Sembay S., Turner M. J. L., Warwick R., 2001, ApJ, 554, 274
Elvis M. et al., 1994, ApJS, 95, 1
Falcke H., Patnaik A. R., Sherwood W., 1996, ApJ, 473, L13
Farrah D., Lacy M., Priddey R., Borys C., Afonso J., 2007, ApJ, 662, L59
Fossati G. et al., 2000, ApJ, 541, 153
Gallagher S. C., Everett J. E., 2007, in Ho L. C., Wang J.-M., eds, ASP Conf. Ser. Vol. 373, The Central Engine of Active Galactic Nuclei. Astron. Soc. Pac., San Francisco, p. 305
Gallagher S. C., Brandt W. N., Chartas G., Garmire G. P., 2002a, ApJ, 567, 37
Gallagher S. C., Brandt W. N., Chartas G., Garmire G. P., Sambruna R. M., 2002b, ApJ, 569, 655
Gallagher S. C., Brandt W. N., Chartas G., Priddey R., Garmire G. P., Sambruna R. M., 2006, ApJ, 644, 709

Gallagher S. C., Hines D. C., Blaylock M., Priddey R. S., Brandt W. N., Egami E. E., 2007, ApJ, 665, 157
Ganguly R., Brotherton M. S., 2008, ApJ, 672, 102
Ganguly R., Brotherton M. S., Cales S., Scoggins B., Shang Z., Vestergaard M., 2007, ApJ, 665, 990
George I. M., Turner T. J., Yaqoob T., Netzer H., Laor A., Mushotzky R. F., Nandra K., Takahashi T., 2000, ApJ, 531, 52
Ghisellini G., Padovani P., Celotti A., Maraschi L., 1993, ApJ, 407, 65
Ghisellini G., Tavecchio F., Foschini L., Ghirlanda G., Maraschi L., Celotti A., 2010, MNRAS, 402, 497
Ghosh K. K., Punsly B., 2007, ApJ, 661, L139
Giommi P. et al., 2012, A&A, 541, A160
Green P. J., Mathur S., 1996, ApJ, 462, 637
Green P. J. et al., 2009, ApJ, 690, 644
Gregg M. D., Becker R. H., de Vries W., 2006, ApJ, 641, 210
Gregory P. C., Condon J. J., 1991, ApJS, 75, 1011
Grupe D., Mathur S., Elvis M., 2003, AJ, 126, 1159
Hall P. B. et al., 2002, ApJS, 141, 267
Hamann F., Korista K. T., Morris S. L., 1993, ApJ, 415, 541
Hewett P. C., Foltz C. B., 2003, AJ, 125, 1784
Hewett P. C., Foltz C. B., Chaffee F. H., 1995, AJ, 109, 1498
Hewett P. C., Foltz C. B., Chaffee F. H., 2001, AJ, 122, 518
Jiang D. R., Wang T. G., 2003, A&A, 397, L13
Jorstad S. G. et al., 2010, ApJ, 715, 362
Kataoka J., Takahashi T., Makino F., Madejski G. M., Tashiro M., Urry C. M., Kubo H., 2000, ApJ, 528, 243
Landt H., Padovani P., Giommi P., Perri M., Cheung C. C., 2008, ApJ, 676, 87
Lazarova M. S., Canalizo G., Lacy M., Sajina A., 2012, ApJ, 755, 29
Lewis G. F., Chapman S. C., Kuncic Z., 2003, ApJ, 596, L35
Marscher A. P. et al., 2008, Nat, 452, 966
Marscher A. P. et al., 2010, ApJ, 710, L126
Marshall H. L. et al., 2005, ApJS, 156, 13
Miller B. P., Brandt W. N., Gallagher S. C., Laor A., Wills B. J., Garmire G. P., Schneider D. P., 2006, ApJ, 652, 163
Miller B. P., Brandt W. N., Gibson R. R., Garmire G. P., Shemmer O., 2009, ApJ, 702, 911
Morrison R., McCammon D., 1983, ApJ, 270, 119
Najita J., Dey A., Brotherton M., 2000, AJ, 120, 2859
Ogle P. M., Cohen M. H., Miller J. S., Tran H. D., Goodrich R. W., Martel A. R., 1999, ApJS, 125, 1
Page K. L., Reeves J. N., O'Brien P. T., Turner M. J. L., 2005, MNRAS, 364, 195
Punsly B., 2006, ApJ, 647, 886
Reynolds C., Punsly B., O'Dea C. P., 2013, ApJ, 773, L10
Richards G. T. et al., 2006, ApJS, 166, 470
Sambruna R. M., Gliozzi M., Donato D., Maraschi L., Tavecchio F., Cheung C. C., Urry C. M., Wardle J. F. C., 2006, ApJ, 641, 717
Sambruna R. M., Donato D., Tavecchio F., Maraschi L., Cheung C. C., Urry C. M., 2007, ApJ, 670, 74
Shankar F., Dai X., Sivakoff G. R., 2008, ApJ, 687, 859
Sprayberry D., Foltz C. B., 1992, ApJ, 390, 39
Steffen A. T., Strateva I., Brandt W. N., Alexander D. M., Koekemoer A. M., Lehmer B. D., Schneider D. P., Vignali C., 2006, AJ, 131, 2826
Stocke J. T., Morris S. L., Weymann R. J., Foltz C. B., 1992, ApJ, 396, 487
Streblyanska A., Barcons X., Carrera F. J., Gil-Merino R., 2010, A&A, 515, A2
Takahashi T. et al., 1996, ApJ, 470, L89
Tozzi P. et al., 2006, A&A, 451, 457
Wang T.-G., Zhou H.-Y., Wang J.-X., Lu Y.-J., Lu Y., 2006, ApJ, 645, 856
Wang J., Jiang P., Zhou H., Wang T., Dong X, Wang H., 2008, ApJ, 676, L97
York D. G. et al., 2000, AJ, 120, 1579
Zhou H., Wang T., Wang H., Wang J., Yuan W., Lu Y., 2006, ApJ, 639, 716


This paper has been typeset from a TEX/LATEX file prepared by the author.